Elaboration of chalcogenide microstructured optical fibers preform by 3D additive manufacturing

Julie Carcreff, François Cheviré, Elodie Galdo, Ronan Lebullenger, Antoine Gautier, Jean-Luc Adam, David Le Coq, Laurent Brilland, Radwan Chahal, Gilles Renversez, et al.

Elaboration of chalcogenide microstructured optical fibers preform by 3D additive manufacturing

Julie Carcreff [a], François Cheviré [a], Elodie Galdo [a], Ronan Lebullenger [a], Antoine Gautier [a], Jean-Luc Adam [a], David Le Coq [a], Laurent Brilland [b], Radwan Chahal [b], Gilles Renversez [c], and Johann Troles*[a]

[a] Univ Rennes, CNRS, ISCR-UMR 6226, F-35000 Rennes, France

[b] Selenoptics, 263 Avenue Gal Leclerc, 35042 Rennes, France

[c] Aix–Marseille Univ, CNRS, Centrale Marseille, Institut Fresnel, UMR 7249, 13013 Marseille,

ABSTRACT

For several years, chalcogenide glasses have been studied as good candidates for numerous applications in the mid-infrared region. Indeed, these glasses are transparent from 1 to 20 µm (depending on the composition), a mid- IR windows well-suited for sensing molecules whose optical signatures are located in the 2-16 µm range. In addition, thanks to appropriate thermal properties, chalcogenide glasses can be drawn into fibers, including microstructured optical fibers.

In this work, a new method based on 3D-printing process is investigated to produce hollow chalcogenide glass preforms, which are then drawn into hollow-core fibers. The transmission of the "printed" hollow-core fiber has been measured and compared to the initial glass. A significant, but still manageable, increase by a factor of 2.5 is observed. This works opens a promising way for the fabrication of chalcogenide MOFs, more particularly for the elaboration of hollow core fibers.

Keywords: chalcogenide glasses, microstructured optical fibers, 3D printing

1. INTRODUCTION

In recent years, the interest for optical materials and fibers operating in the mid infrared (mid-IR) region has grown tremendously. This interest originates from societal needs in the fields of health and environment for instance, and also from demand for defense applications. Indeed, the mid-IR spectral region contains the atmospheric transparent windows (3-5 µm) and (8-12 µm) where thermal imaging (military and civilian) can take place. Furthermore, the infrared window is well-suited for sensing (bio)-molecules, whose fingerprints are located at wavelengths between 2 and 15 µm. In this context, the development of mid-IR transparent materials and optical fibers is essential. Chalcogenide glasses are good candidates for the realization of new and innovative mid-IR systems. Thus, chalcogenide fibers have been utilized for versatile mid-IR fiber transmission [1, 2], supercontinuum generation [3, 4], and sensing [5, 6, 7].

An original way to obtain single-mode fibres is to design microstructured optical fibres (MOFs). Such fibers present unique optical properties thanks to the high degree of freedom in the design of their geometrical structure. Since the primary works on silica MOFs, this new class of fibres has attracted much interest in the optical fibre community [8]. Different methods for the realization of chalcogenide preforms and microstructured fibers have been reported, such as the stack and draw method [9, 10], drilling method [11, 12, 13], extrusion processes [14, 15] and molding method [16, 17].

In this context, we have investigated an alternative way for fabricating microstructured preforms by using an original 3D printing process. By using this additive manufacturing method, preforms with complex designs can be fabricated in a single step within a couple of hours, with a high degree of repeatability and precision of the geometry. The cost of fabrication can be reduced as well, as compared to traditional techniques. Till now, no 3D printing preform made with chalcogenide glasses has been reported. Only bulk As_2S_3 has been obtained by an additive manufacturing process [18]. In this study, the fabrication of a holey chalcogenide preform is reported for the first time. A holey fiber has been drawn from the preform, and transmission of infrared light has been demonstrated. Finally, the optical attenuation of the printed fiber has been compared to the one of a chalcogenide fiber drawn from a standard melt-quenched preform.

2. THE CHOSEN CHALCOGENIDE GLASS: $TE_{20}AS_{30}SE_{50}$

Besides being transparent in the mid-infrared, the chalcogenide glass to be chosen must be compatible with the constraints of standard thermal 3D printing process.

First, the glass transition temperature (T_g) of the glass has to be lower than 300 °C, which the maximum temperature that can be reach by commercial 3D printing extrusion heads used for polymer. Second, the glass has to be strongly stable against crystallisation to avoid crystallisation during printing of the preform. The $Te_{20}As_{30}Se_{50}$ (TAS) composition fulfils perfectly these requirements, as shown below.

The TAS glasses were prepared by melt-quenching technique in a evacuated silica ampoule containing the different raw elements Te (5N), As (5N) and Se (5N). The ampoule is then heated in a rocking furnace during few hours at 650 °C and finally, the melted glass was quenched at room temperature and placed in an annealing furnace at T_g +10 °C during 3 hours and then slowly cooled to the room temperature.

2.1 Thermal properties of TAS Glass

Calorimetric measurements were carried out with a differential scanning calorimeter (DSC). The glass transition temperature (T_g) was determined by heating 10 mg of a TAS sample in a hermetic aluminium pan at 10 °C/min rate. T_g was measured at around 137 °C, as shown in figure 1. In addition, no crystallization peak has been observed up to 280 °C, which demonstrates the stability of the glass against crystallisation.

Viscosity measurements have been carried out by means of a parallel-plates experimental set-up. The lower viscosity than can be measured with this set-up is 10^4 Pa.s. The results are displayed in figure 2. By extrapolating with VFT equation the curve, a range of viscosity of 10-10^3 Pa.s can be estimated between 260 °C and 300 °C, which correspond to the conventional viscosities and temperatures used for standard thermal 3D printing of polymers [19]. As a result, one can assume that the additive manufacturing method can be implemented with TAS glass.

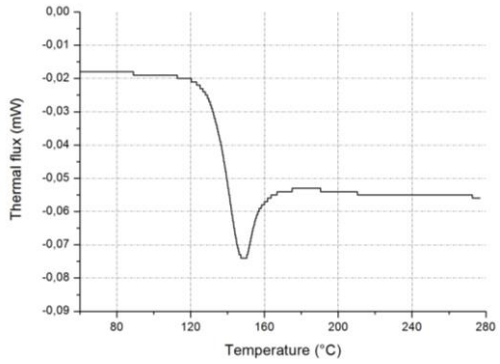

Figure 1. DSC Curve of TAS chalcogenide glass

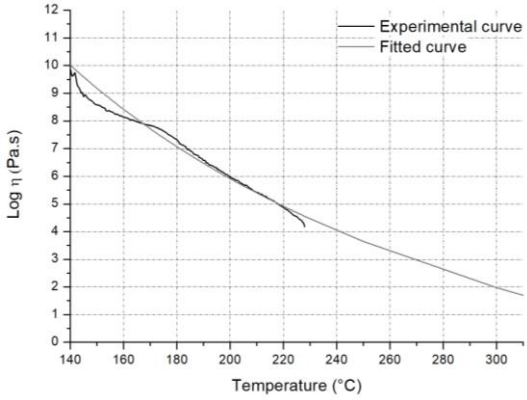

Figure 2. Viscosity curve of TAS glass

2.2 Optical properties

The main goal of this study is to explore a new way for the elaboration of chalcogenide MOFs, and more particularly for fabricating hollow-core fibers. Preliminary modelling works have been carried out in order to define the optimized design of the future fiber. For defining the best fiber geometry, optical properties of TAS glass, such as the refractive index and fiber attenuation, have to be taken into account. Figure 3 presents the values of TAS glass refractive index as a function of wavelength. The refractive index varies from 2.96 (at 2 µm) to 2.90 (at 12 µm) [20]. The typical attenuation curve of a high purity TAS glass is presented in figure 4. The optical losses are less than 3 dB/m between 3 and 10 µm and less than 100 dB/m between 1 and 17 µm. Thanks to preliminary modelisations, we can expect an attenuation less than 10 dB/km at 10 µm in a TAS hollow core fiber.

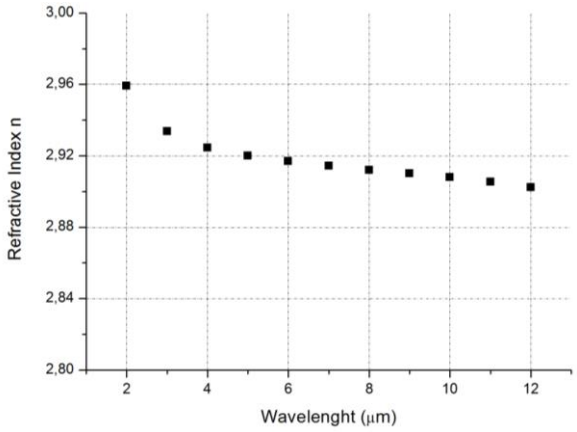

Figure 3. Refractive index of TAS glass in the mid-IR [20]

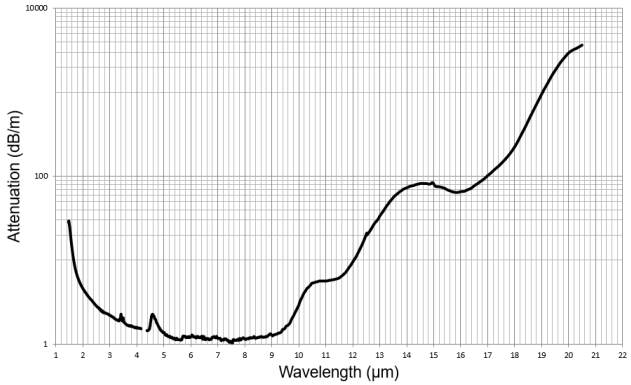

Figure 4. Typical attenuation curve of a high purity TAS glass

3. CHALCOGENIDE GLASSES 3D PRINTING PROCESS

3.1 Homemade 3D printer

The principles of 3D printing can be found in Ref. [21]. In this study, the 3D-printing set-up is based on a customized commercial RepRap-style 3D printer (Anet A8) upgraded for soft glasses. Especially, the feeding mechanism is customized for brittle materials. This mechanism is supplied with 400-mm long TAS rods with 1.75 to 3-mm diameters, produced by the fiber-drawing method. An extruder drives the raw material filament to a nozzle, heated well above T_g. The printer head moves in the X and Z directions and the bed plate in Y direction while depositing the TAS glass as a thin layer on the pan. The nozzle can control the diameter of the extruded filament from 250 µm to 400 µm.

The printer head, made in copper, can reach an extrusion temperature of 400 °C. As shown in figure 2, TAS glass reaches a suitable viscosity when the temperature is above 250 °C. In consequence, the temperature of the printer head and the nozzle was fixed at 300 °C. The size of the nozzle, and consequently, the thickness of the printed lines were

about 400 µm. The TAS glass was deposited on a sodalime glass bed plate heated around 140 °C, which ensures a good adherence of the printed sample.

At the end, a TAS glass bulk pellet of 5 mm height and 10 mm diameter was obtained.

3.2 Characterization of the "printed" glass

The printed glass pellet was polished before being analyzed.

Scanning electron microscopy (SEM) images are presented in figure 5. Some filaments and lines are visible on the external surface of the printed disk (figure 5a). However, no significant defects are observed inside the TAS printed pellet which cut in two pieces in order to observe the quality of glass (figure 5b). That means that a good adhesion between different layers has been obtained.

The composition of the pellet was analyzed and evaluated by Energy Dispersive Spectroscopy (EDS), as shown in Table 1. Comparison with the initial composition of the glass, indicates that there is no composition change of the glass during the printing process, within the experimental error. In addition, one can note that from EDS analysis no contamination such as contamination from the printer head and/or the nozzle is observed.

The glass transition temperature (T_g), the optical transmission and the density of the printed TAS glass have been also compared to a bulk TAS glass obtained by the standard melting-quenching process (see table 2 and figure 6). Once again, if one considers the experimental error inherent in DSC measurements, the T_g's of the printed glass and the initial glass are the same. Also, no crystallization peak has been observed in the DSC measurement of the printed glass.

The transmission spectra of the printed and initial TAS glasses are similar in terms of spectral domain. However, the maximum of transmission of the extruded TAS is limited to 20 %, to be compared to 65 % for the initial glass. That indicates the presence of numerous scattering defects in the printed pellet, even though no significant defects were observed in the SEM image. The decrease of density for the printed glass, as reported in table 2 suggests the presence of numerous bubbles, which could be responsible for the strong decrease of transmission observed for the printed glass.

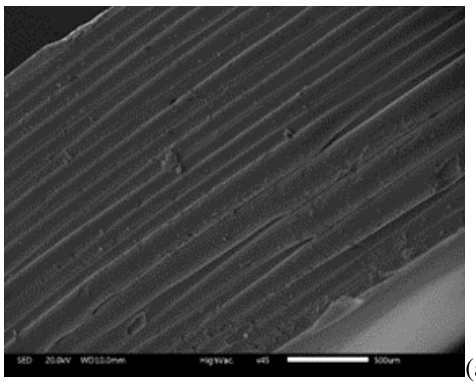
(a)
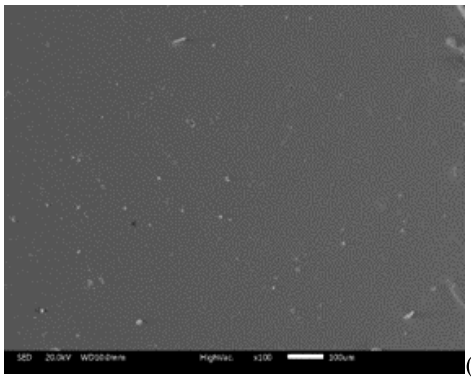
(b)

Figure 5. SEM Image of external side of cylinder and internal TAS printed bulk

Table 1. Results of EDS analysis for initial and printed bulk TAS glasses

	Initial glass composition (%)	**Printed glass composition (%)**
Te	20	21
As	30	29
Se	50	50

At this stage, one can conclude that the chemical composition and thermal properties of TAS glass remain unchanged before and after the printing process. However, the printed material seems to present numerous scattering defects, especially bubbles.

Table 2. Comparison of physical properties of the $Te_{20}As_{30}Se_{50}$ initial glass and printing glass.

T_g (°C)	Transmission Range (µm)	Density ($g.cm^{-3}$)	Refractive index at 2 µm
137	2-18	4.864	2.95
136	2-18	4.632	-

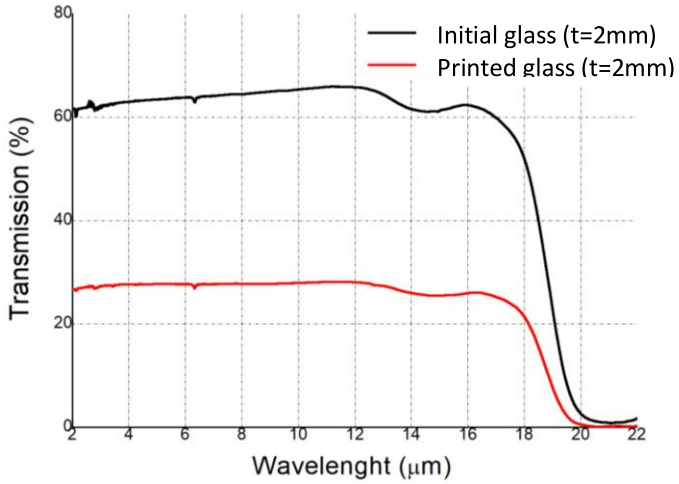

Figure 6. Bulk transmission comparison between printed bulk glass and melt-quenched glasses

4. "PRINTED" OPTICAL FIBERS

After printing small bulk pellets, the printing of a holey cylinder, or preform, with a 8-mm outer diameter and 3.2-mm internal diameter has been carried out. The deposition of successive layers permits to reach a preform length close to 15 mm. The printing has been interrupted due to a lack of raw material from the feeding machine. The cylinder obtained is shown in figure 7a and the surface of the cylinder, observed by an optical microscope, is shown in figure 7b. Streaks related to the deposition of the material layer by layer are clearly visible, but they do not impair the mechanical cohesion of the piece. The cylinder is not friable.

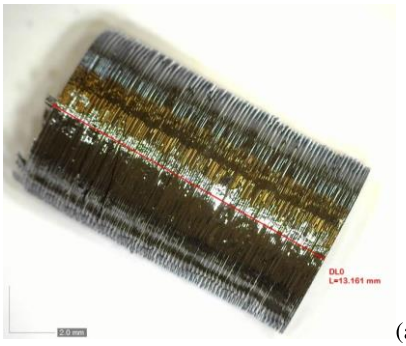
(a)

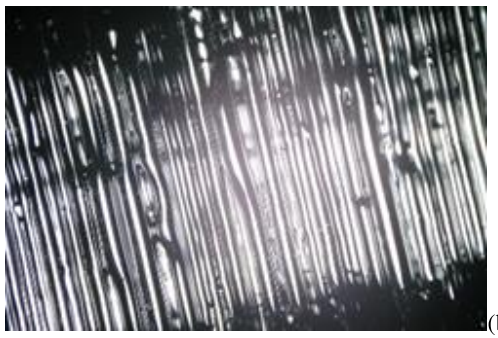
(b)

Figure 7. Microscope images of the side external surfaces of the printed cylinder

Then, the 15 mm-high preform has been drawn. The major difficulty was to draw such a short preform. However, a couple of meters of fiber could be obtained with an outer diameter of around 400 µm. This fibre is the first fiber ever obtained by drawing a printed chalcogenide glass preform.

The cross section and the outer surface quality of the "printed" fiber are presented in figure 8. The surface image reveals the presence of numerous bubbles, appearing as small black dots, and shows a significant distortion of the initial geometry, impairing mainly the centering and shape of the central hole. Nevertheless, the surface does not show any major defects. Indeed, the streaks observed on the surface of the preform in figure 7 are totally smoothed by the fiber drawing process

Attenuation measurements have been performed in order to compare the optical transmission of the intial glass fiber and the "printed" fiber. The results are shown in figure 9. A significant increase of the optical losses is observed for the "printed" fiber. Thus, when the minimum of attenuation of the initial glass is less than 10 dB/m, the minimum of attenuation of the "printed" fiber is measured at around 25 dB/m. This important decrease of the optical quality of the glass is mainly due to the presence of numerous scattering defects like bubbles, as observed in the cross section of the fiber (figure 8).

Furthermore, new absorption peaks appear in the attenuation curve of the printed fiber, mainly due to contamination by water, oxygen and carbon during the 3D printing process. These pollutions are not surprising considering that printing is carried out in air.

One can note that the initial glass was not a purified glass that explaining the discrepancy between the attenuation curves of the TAS glass shown in the figure 4 and 10. The optical quality of the printed fibres could be strongly improved by using a feeding rod made of high purity TAS glass and by implementing the printing process under neutral atmosphere.

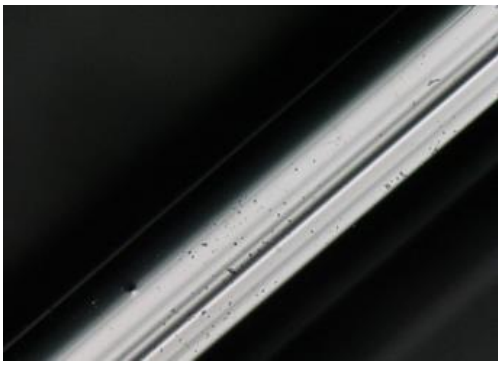

Figure 8. Microscope images of the outer surface of the TAS fiber drawn from a printed preform

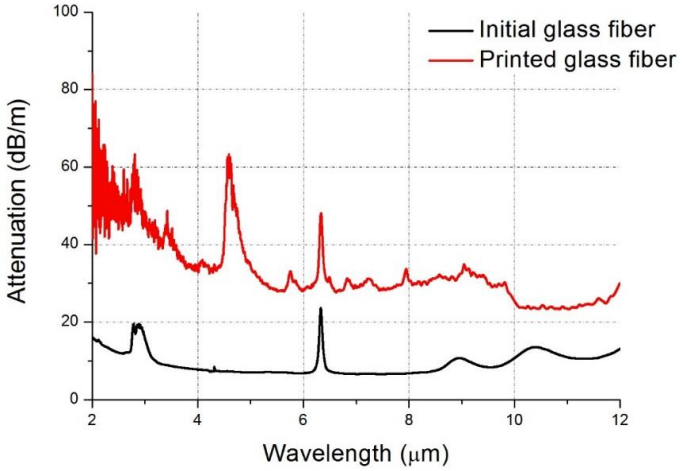

Figure 9. Attenuation of the "printed" TAS holey fiber and initial fiber

5. CONCLUSION

In conclusion, the proof of concept of 3D printing of a chalcogenide glass has been demonstrated. Furthermore, a chalcogenide preform has been obtained by this original additive manufacturing process, and such preform has been drawn into optical fibers. This first ever chalcogenide "printed" fiber show optical losses of 25-40 dB/m in the 4-12 µm window, which could be strongly improved by using high optical quality raw glasses and by printing the preforms under controlled atmosphere.

Those results open a new way for the elaboration of chalcogenide MOFs, especially for the preparation of hollow-core chalcogenide MOFs.

6. ACKNOWLEDGE

This work was funded in part by the European Union through the European Regional Development Fund (ERDF), the Ministry of Higher Education and Research, the french region of Brittany, Rennes Métropole, the French National Research agency and DGA (grant ANR ASTRID DGA FOM-IR-2-20).

REFERENCES

[1] Shiryaev V. S. et al., « Single-mode infrared fibers based on TeAsSe glass system », Materials Science and Engineering: B 127, n° 2: 138-43 (2006).
[2] Tao G. et al., « Infrared Fibers », Advances in Optics and Photonics 7, n° 2: 379-458 (2015).
[3] Dai S. et al., « A Review of Mid-Infrared Supercontinuum Generation in Chalcogenide Glass Fibers », Applied Sciences 8, n° 5: 707 (2018).
[4] Wu Y. et al., « Chalcogenide Microstructured Optical Fibers for Mid-Infrared Supercontinuum Generation: Interest, Fabrication, and Applications », Applied Sciences 8, n° 9: 1637 (2018).
[5] Brandily M. L. et al., « Identification of foodborne pathogens within food matrices by IR spectroscopy », Sensors and Actuators B: Chemical 160, n° 1: 202-6 (2011).
[6] Toupin P. et al., « Comparison between chalcogenide glass single index and microstructured exposed-core fibers for chemical sensing », Journal of Non-Crystalline Solids, ISNOG 2012 Proceedings of the 18th International Symposium on Non-Oxide and New Optical Glasses Rennes, France, July 1-5, 2012, 377, 217-19 (2013).
[7] Seddon A. B. et al., « Prospective on Using Fibre Mid-Infrared Supercontinuum Laser Sources for in Vivo Spectral Discrimination of Disease », Analyst 143, n° 24: 5874-87 (2018).
[8] Birks T.A. et al., « Full 2-D photonic bandgaps in silica/air structures », Electronics Letters 31, n° 22: 1941-43 (1995).
[9] Desevedavy F. et al., « Chalcogenide glass hollow core photonic crystal fibers », Optical Materials 32, n° 11: 1532-39 (2010).
[10] Brilland L. et al., « Interfaces impact on the transmission of chalcogenides photonic crystal fibres », Journal of the Ceramic Society of Japan 116, n° 1358: 1024-27 (2008).
[11] Zhang P. et al., « Fabrication of chalcogenide glass photonic crystal fibers with mechanical drilling », Optical Fiber Technology 26: 176-79 (2015).
[12] El-Amraoui M. et al., « Microstructured Chalcogenide Optical Fibers from As_2S_3 Glass: Towards New IR Broadband Sources », Optics Express 18, n° 25: 26655-65 (2010).
[13] Yuan Y. et al., « Precision Fabrication of a Four-Hole $Ge_{15}Sb_{15}Se_{70}$ Chalcogenide Suspended-Core Fiber for Generation of a 1.5µm Ultrabroad Mid-Infrared Supercontinuum », Optical Materials Express 9, n° 5: 2196-2205 (2019).
[14] Xue Z. et al., « Infrared Suspended-Core Fiber Fabrication Based on Stacked Chalcogenide Glass Extrusion », Journal of Lightwave Technology 36, n° 12: 2416-21 (2018).
[15] Wu B. et al., « Mid-Infrared Supercontinuum Generation in a Suspended-Core Tellurium-Based Chalcogenide Fiber », Optical Materials Express 8, n° 5: 1341-48 (2018).
[16] Coulombier Q. et al., « Casting Method for Producing Low-Loss Chalcogenide Microstructured Optical Fibers », Optics Express 18, n° 9: 9107-12 (2010).

[17] Toupin P. et al., « Small Core Ge-As-Se Microstructured Optical Fiber with Single-Mode Propagation and Low Optical Losses », Optical Materials Express 2, n° 10: 1359-66 (2012).
[18] Baudet E. et al., « 3D-Printing of Arsenic Sulfide Chalcogenide Glasses », Optical Materials Express 9, n° 5 (2019).
[19] Brydson J. A., Plastics Materials (Elsevier, 1999).
[20] Houizot P. et al., « Infrared Single Mode Chalcogenide Glass Fiber for Space », Optics Express 15, n° 19: 12529-38 (2007),
[21] Ngo T. D. et al., « Additive manufacturing (3D printing): A review of materials, methods, applications and challenges », Composites Part B: Engineering 143: 172-96 (2018).